Unveiling the heavy neutrino nature at LHCb

G. A. Vasquez[1,*] and Jilberto Zamora-Saa[2,3,†]

[1]*Department of Physics and Astronomy, University of Victoria, Victoria, British Columbia V8P 5C2, Canada*
[2]*Center for Theoretical and Experimental Particle Physics, Facultad de Ciencias Exactas, Universidad Andres Bello, Fernandez Concha 700, Santiago, Chile*
[3]*Millennium Institute for Subatomic Physics at High Energy Frontier—SAPHIR, Fernandez Concha 700, Santiago, Chile*

(Received 11 July 2023; accepted 6 September 2023; published 21 September 2023)

In this work, we study the lepton number violating B_c meson decays via one intermediate on-shell heavy neutrino N. The specific studied process is $B_c^+ \to \mu^+ N \to \mu^+\mu^+\tau^-\nu$ which could allow distinguishing the nature of the heavy neutrino nature (Dirac or Majorana) by studying the tau lepton energy spectrum in the LHCb experiment. The result suggests that this signature could be observed in the collected data during the HL-LHCb lifetime.

DOI: 10.1103/PhysRevD.108.053008

I. INTRODUCTION

The standard model (SM) of physics is a highly successful theoretical framework that encompasses the fundamental particles and forces of nature, encompassing quarks, leptons, and bosons. However, there are various phenomena in the universe that the standard model fails to explain. These include the baryonic asymmetry of the universe (BAU), dark matter (DM), and neutrino oscillations (NOs). Over the past few decades, experiments on NOs have demonstrated that active neutrinos (ν) are massive particles setting limits on the squared mass difference $\Delta m^2 = 10^{-10}$ eV^2 (from solar neutrino experiments), $\Delta m^2 = 10^{-2} - 10^{-3}$ eV^2 (from short baseline reactor experiments), $\Delta m^2 = 10^{-4} - 10^{-5}$ eV^2 (from long baseline reactor experiments), $\Delta m^2 > 0.1$ eV^2 (from short baseline accelerator experiments) and $\Delta m^2 = 10^{-2} - 10^{-3}$ eV^2 (from long baseline accelerator experiments), see Ref. [1] for more details. Consequently, it is evident that the standard model is not a final theory and necessitates expansion. Among the extensions to the standard model, which provide an explanation for the minuscule masses of active neutrinos, are those rooted in the seesaw mechanism (SSM) [2,3]. This mechanism introduces a heavy Majorana neutral lepton, commonly referred to as the heavy neutrino (HN), which is a singlet under the $SU(2)_L$ symmetry group. The presence of the HN ultimately leads to the existence of a very light active Majorana neutrino. These hypothetical HN's have strongly suppressed interaction with the SM particles ($Z, W^\pm$ bosons and e, μ, τ leptons), doing a very tough task their detection. However, despite this suppression, the existence of HN's can be explored via rare meson decays [4–17], colliders [18–38], and tau factories [39–41].

A well-motivated extension of the Standard Model (SM) known as the neutrino-minimal-Standard-Model (νMSM) [42,43] has been proposed. The νMSM is based on the seesaw mechanism (SSM) and introduces three heavy neutrinos. Among these, two HN's have nearly identical masses of around 1 GeV (denoted as m_{N1} and m_{N2}), while the third one has a mass of approximately keV and is considered a candidate for dark matter. In addition to explaining the smallness of neutrino masses and neutrino oscillations, the νMSM has cosmological implications for the early universe. It can generate a slight imbalance between matter and antimatter through a phenomenon called heavy neutrino oscillations (HNOs), which is also known as the Akhmedov-Rubakov-Smirnov (ARS) mechanism [44].

In a previous publication [45], we provided an explanation of the impacts arising from HNOs in the rare decays of pseudoscalar B mesons, specifically those violating lepton number (LNV) and lepton flavor (LFV). These decays involve two nearly indistinguishable heavy Majorana neutrinos ($m_{N_i} \sim 1$ GeV), which can undergo oscillations among themselves. The objective of this article is to introduce a technique that facilitates the identification of the heavy neutrino at HL-LHCb by utilizing the remarkable detector resolution [46,47], thereby enabling the potential observation of HNOs.

*g.vasquez@cern.ch
Currently at the Physiks Department of University of Zurich.
†jilberto.zamorasaa@cern.ch, jilberto.zamora@unab.cl

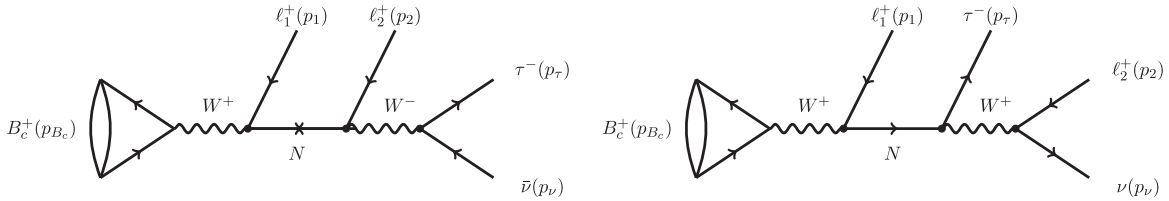

FIG. 1. The rare B_c^+ meson decay, intermediated by a heavy neutrino. Left: Feynman diagrams for the LNV process $B_c^+ \to \ell_1^+ \ell_2^+ \tau^- \bar{\nu}$. Right: Feynman diagrams for the LNC process $B_c^+ \to \ell_1^+ \tau^- \ell_2^+ \nu$. In this study, we will focus on a scenario where $\ell_1 = \ell_2 = \mu$.

The work is arranged as follows: In Sec. II, we described the production of heavy neutrinos mechanism in B_c meson decays. In Sec. III, we discuss the simulations of the HN production at LHCb. In Sec. IV, we present the summary and shows the conclusions.

II. PRODUCTION OF HEAVY NEUTRINOS

As we stated in the introduction, we are interested in studying the lepton number violating (LNV) and the lepton number conserving (LNC) in rare B_c meson decay processes, the same signature could be studied in B meson decays, however, the suppression due to CKM elements is stronger, leading to the B_c decays be a better option (see Ref. [8] for a deeper discussion). The LNV process can be intermediated only by Majorana HN, while the LNC by Majorana and Dirac HN (see Fig. 1). The decay width for the studied processes, in terms of 4-body invariant phase space $d_4(B_c^+ \to \mu^+\mu^+\tau^-\bar{\nu})$ in terms of the squared amplitude $|\mathrm{A}_\mathrm{X}^+|^2$, and for the HN kinematically allowed mass range $(m_\tau + m_\mu) \leq m_N \leq (m_{B_c} - m_\mu)$ is

$$\Gamma_\mathrm{X}(B_c^+ \to \mu^+\mu^+\tau^-\bar{\nu}) = \frac{1}{2m_{B_c}(2\pi)^8} \int d_4(B_c^+ \to \mu^+\mu^+\tau^-\bar{\nu}) |\mathrm{A}_\mathrm{X}^+|^2, \quad (1)$$

where $\mathrm{X} = \mathrm{LNC}$ or $\mathrm{X} = \mathrm{LNV}$. The squared amplitudes in terms of particles 4-momenta and the propagators are given by

$$|\mathrm{A}_\mathrm{LNV}^+|^2 = 256 G_F^4 |V_{cb}|^2 f_{B_{cb}}^2 |T_\mathrm{LNV}|^2 (p_2 \cdot p_\nu)[2(p_1 \cdot p_{B_c})(p_\tau \cdot p_{B_c}) - m_{B_c}^2 (p_1 \cdot p_\tau)]$$

$$|\mathrm{A}_\mathrm{LNC}^+|^2 = 256 G_F^4 |V_{cb}|^2 f_{B_{cb}}^2 |T_\mathrm{LNC}|^2 (p_\tau \cdot p_\nu)(2m_1^2 (p_2 \cdot p_{B_c})[m_{B_c}^2 - (p_1 \cdot p_{B_c})] \quad (2)$$

$$\times (p_1 \cdot p_2)[m_{B_c}^4 - m_{B_c}^2 m_1^2 + 4(p_1 \cdot p_{B_c})^2 - 4m_{B_c}^2 (p_1 \cdot p_{B_c})]), \quad (3)$$

where the propagators are

$$T_\mathrm{LNC} = \frac{B_{\tau N} B_{\mu N}^*}{P_N^2 - m_N^2 + i\Gamma_N^\eta m_N}; \quad T_\mathrm{LNV} = \frac{m_N B_{\mu N}^* B_{\mu N}^*}{P_N^2 - m_N^2 + i\Gamma_N^\eta m_N}. \quad (4)$$

The factors $f_{B_{cb}} = 0.322$ GeV [48] and $V_{cb} = 0.041$ [49] correspond to the decay constant and the CKM matrix element for B_c meson, respectively. In Eq. (4), the factor Γ_N^η is the total heavy neutrino decay width, which in principle, can be different for Dirac ($\eta = \mathrm{Dir}$) and Majorana ($\eta = \mathrm{Maj}$) heavy neutrinos

$$\Gamma_N^\eta \equiv \Gamma^\eta(m_N) \approx \mathcal{K}^\eta \frac{G_F^2 m_N^5}{96\pi^3}, \quad (5)$$

here $G_F \approx 1.166 \times 10^{-5}$ GeV^{-2} [50] is the Fermi coupling constant. The factor $\mathcal{K}^\eta$ is given by

$$\mathcal{K}^\eta = \mathcal{N}_e^\eta |B_{eN}|^2 + \mathcal{N}_\mu^\eta |B_{\mu N}|^2 + \mathcal{N}_\tau^\eta |B_{\tau N}|^2, \quad (6)$$

where the factors $B_{\ell N}$ are the heavy-light mixing elements of the Pontecorvo-Maki-Nakagawa-Sakata matrix[1] which in this work are set to $|B_{eN}|^2 = 1 \times 10^{-8}$, $|B_{\mu N}|^2 = 5 \times 10^{-7}$ and $|B_{\tau N}|^2 = 5 \times 10^{-6}$ all of these widely allowed[2] by current limits [51,52], the factors $\mathcal{N}_\ell^\eta$ are the effective mixing coefficients which account for all possible decay

[1] In this work we define the light neutrino flavor state as $\nu_\ell = \sum_{i=1}^3 U_{\ell i}\nu_i + B_{\ell N} N$. Nevertheless, other literature uses $U_{\ell N}$ or $V_{\ell N}$ as the heavy-light mixings elements (i.e., $B_{\ell N} \equiv U_{\ell N} \equiv V_{\ell N}$).

[2] It is important to mention that in the experimental mixing limits $|B_{\ell N}|^2$ presented in Refs. [4,51,52] several discovery channels have been taken into account. Therefore, when we have set our mixings limits to $|B_{eN}|^2 = 1 \times 10^{-8}$, $|B_{\mu N}|^2 = 5 \times 10^{-7}$, and $|B_{\tau N}|^2 = 5 \times 10^{-6}$ we are in a conservative scenario due to our mixings are widely allowed by current limits which read $|B_{eN}|^2 < 1 \times 10^{-6}$, $|B_{\mu N}|^2 = 1 \times 10^{-6}$, and $|B_{\tau N}|^2 = 1 \times 10^{-5}$ for $2 \leq m_N \leq 4$ GeV.

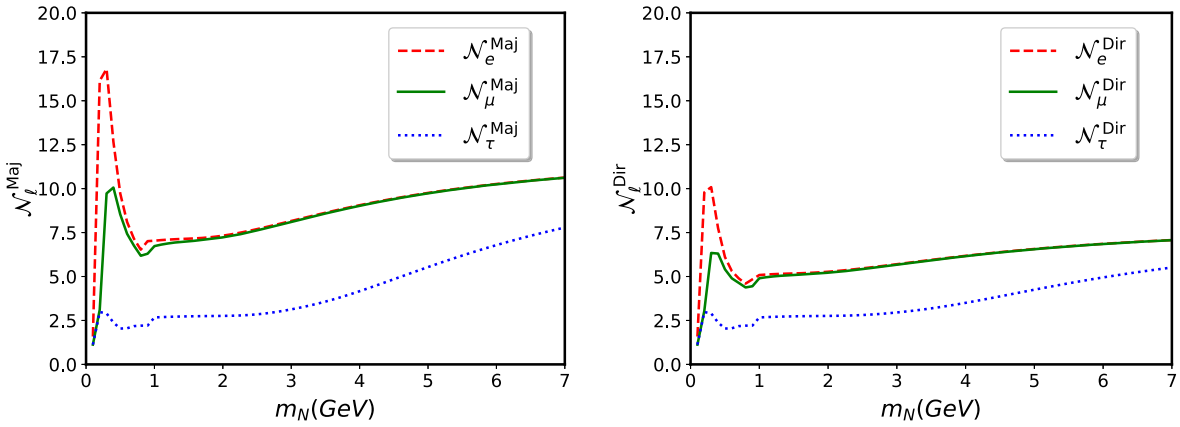

FIG. 2. The effective mixing coefficients $\mathcal{N}_\ell^\eta$. Left: $\mathcal{N}_\ell^{\rm Maj}$ for Majorana heavy neutrinos. Right: $\mathcal{N}_\ell^{\rm Dir}$ for Dirac heavy neutrinos. Figure adapted from Ref. [8].

channels of N (see Appendix B in Ref. [8] for a detailed explanation) and are presented in Fig. 2 for our HN mass of interest ($0 \leq m_N \leq 7.0$ GeV).

Due to the different 4-momenta structure between $|A^+_{\rm LNV}|^2$ and $|A^+_{\rm LNV}|^2$ [see Eq. (3)], it is possible to infer that the energy spectra of the final tau lepton is an appropriate variable to distinguish the HN nature (see Refs. [6,9] for a detailed discussion). The τ lepton energy spectra, in the heavy neutrino rest frame [CM(N)], for the LNV process is given by

$$\frac{dBr^{(\rm LNV)}(B_c^+ \to \ell_1^+ \ell_2^+ \tau^- \bar{\nu})}{dE_\tau d\cos\theta_\tau} = \frac{Z^{(\rm LNV)}}{\Gamma(B_c \to \text{all})} \frac{[m_N(m_N - 2E_\tau) + m_\tau^2 - m_2^2]^2}{4m_N[m_N(m_N - 2E_\tau) + m_\tau^2]} \times \left\{ \cos\theta_\tau (m_N^2 - m_1^2)\left[(m_{B_c}^2 - m_N^2)^2 - 2m_1^2(m_{B_c}^2 + m_N^2) + m_1^4\right]^{1/2}(E_\tau^2 - m_\tau^2) + \left[m_N^2(m_{B_c}^2 - m_N^2) + m_1^2(m_{B_c}^2 + 2m_N^2) - m_1^4\right] E_\tau \sqrt{E_\tau^2 - m_\tau^2} \right\} + (m_1 \leftrightarrow m_2), \quad (7)$$

where the angle θ_τ is the angle between $\overrightarrow{p_1}$ and $\overrightarrow{p_\tau}$ (see Fig. 3), here both quantities E_τ and θ_τ are in the CM(N) frame, and the function $Z^{(\rm LNV)}$ is defined as

$$Z^{(\rm LNV)} \equiv \left(1 - \frac{1}{2}\delta_{\ell_1,\ell_2}\right) G_F^4 f_{B_c}^2 |B^*_{\ell_1 N} B^*_{\ell_2 N} V^*_{cb}|^2 \times \frac{2}{(2\pi)^4} \frac{m_N}{\Gamma_N^{\rm Maj} m_{B_c}^3} \lambda^{1/2}(m_{B_c}^2, m_N^2, m_1^2), \quad (8)$$

and $\lambda^{1/2}$ is the square root of the function

$$\lambda(x,y,z) \equiv x^2 + y^2 + z^2 - 2xy - 2yz - 2zx. \quad (9)$$

It is important to remark that the factor $(1 - \frac{1}{2}\delta_{\ell_1,\ell_2})$ accounts for the case when $\ell_1 \neq \ell_2$, however in our case $\ell_1 = \ell_2 = \mu$, then $(1 - \frac{1}{2}\delta_{\mu,\mu} = 1/2)$. On the other hand, the term $(m_1 \leftrightarrow m_2)$ accounts for the mass interchange, when ℓ_1 is produced at ℓ_2 vertex and vice-versa (crossed channel). The integration over the angle θ_τ gives

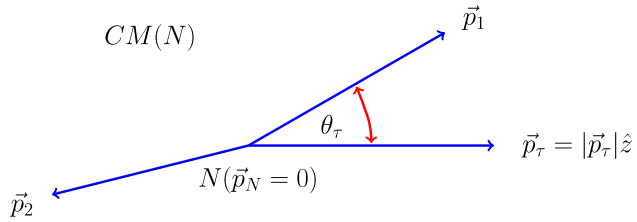

FIG. 3. Scheme of the final 3-momenta in the heavy neutrino rest frame CM(N). For simplicity, we only have represented the relevant angle θ_τ.

$$\frac{dBr^{(\mathrm{LNV})}}{dE_\tau}(B_c{}^+ \to \ell_1^+\ell_2^+\tau^-\overline{\nu}) = \frac{Z^{(\mathrm{LNV})}}{\Gamma(B_c \to \mathrm{all})}\frac{1}{2m_N}\left[m_{B_c}^2(m_N^2+m_1^2)-(m_N^2-m_1^2)^2\right] \times E_\ell\sqrt{E_\tau^2-m_\tau^2}\,\frac{(m_N^2-2m_NE_\tau+m_\tau^2-m_2^2)^2}{(m_N^2-2m_NE_\tau+m_\tau^2)} + (m_1 \leftrightarrow m_2), \tag{10}$$

for the lepton number conserving (LNC) processes we have

$$\begin{aligned}\frac{dBr^{(\mathrm{LNC})}}{dE_\tau d\cos\theta_\tau} = {} & \frac{Z^{(\mathrm{LNC})}}{\Gamma(B_c \to \mathrm{all})}\frac{(-1)\sqrt{E_\tau^2-m_\tau^2}[-m_2^2+m_\tau^2+m_N(m_N-2E_\tau)]^2}{24m_N[m_\tau^2+m_N(m_N-2E_\tau)]^3} \\ & \times\Bigg\{\cos\theta_\tau(m_1^2-m_N^2)\sqrt{E_\tau^2-m_\tau^2}\sqrt{((m_{B_c}+m_1)^2-m_N^2)((m_{B_c}-m_1)^2-m_N^2)} \\ & \times\Big[\big(3m_\tau^2+m_N(m_N-4E_\tau)\big)\big(m_\tau^2+m_N(m_N-2E_\tau)\big)+m_2^2\big(3m_\tau^2-m_N(m_N+2E_\tau)\big)\Big] \\ & +\Big[\big(m_1^4-m_N^2(m_{B_c}^2-m_N^2)-m_1^2(m_{B_c}^2+2m_N^2)\big)\big(8E_\tau^3m_N^2-2m_\tau^2m_N(2m_2^2+m_\tau^2+m_N^2) \\ & +2E_\tau^2m_N(m_2^2+5m_\tau^2+5m_N^2)+E_\tau\big(3m_2^2m_\tau^2+3m_2^2m_N^2+(3m_\tau^2+m_N^2)(m_\tau^2+3m_N^2)\big)\big)\Big]\Bigg\}+(m_1 \leftrightarrow m_2),\end{aligned} \tag{11}$$

where $Z^{(\mathrm{LNC})}$ is defined as

$$Z^{(\mathrm{LNC})} \equiv G_F^4 f_{B_c}^2 |B^*_{\ell_1 N}B_{\tau N}V^*_{cb}|^2\left(1-\frac{1}{2}\delta_{\ell_1,\ell_2}\right)\frac{2}{(2\pi)^4}\frac{m_N}{\Gamma_N^{\mathrm{Dir}}m_{B_c}^3}\lambda^{1/2}(m_{B_c}^2,m_N^2,m_1^2). \tag{12}$$

The integration over θ_τ gives

$$\begin{aligned}\frac{dBr^{(\mathrm{LNC})}}{dE_\tau}(B_c{}^+ \to \ell_1^+\ell_2^+\tau^-\nu) = {} & \frac{Z^{(\mathrm{LNC})}}{\Gamma(B_c \to \mathrm{all})}\frac{1}{96m_N^2}\frac{1}{[m_\tau^2+m_N(-2E_\tau+m_N)]^3} \\ & \times\Bigg\{8\sqrt{(E_\tau^2-m_\tau^2)}m_N\big[m_2^2-m_\tau^2+(2E_\tau-m_N)m_N\big]^2 \\ & \times\big[-m_1^4+m_{B_c}^2m_N^2-m_N^4+m_1^2(m_{B_c}^2+2m_N^2)\big]\big[8E_\tau^3m_N^2-2m_\tau^2m_N(2m_2^2+m_\tau^2+m_N^2) \\ & -2E_\tau^2m_N\big(m_2^2+5(m_\tau^2+m_N^2)\big)+E_\tau\big(3m_\tau^4+10m_\tau^2m_N^2+3m_N^4+3m_2^2(m_\tau^2+m_N^2)\big)\big]\Bigg\} \\ & +(m_1 \leftrightarrow m_2),\end{aligned} \tag{13}$$

An important suppression effect acting on the decay width comes from the finite detector length (L_D), this effect is named acceptance factor (AF^η) and can be written as

$$\mathrm{AF}^\eta = 1-e^{\frac{L_D\Gamma_N^\eta}{\gamma_N\beta_N}}, \tag{14}$$

where $\eta = \mathrm{Dir}, \mathrm{Maj}$, the factor γ_N stands for the HN Lorentz factor, and β_N for the HN velocity, in our analysis, we will use $\gamma_N\beta_N = 2$ (see the Appendix for more details) and $|B_{eN}|^2 = 5\times10^{-7}$ and $|B_{\tau N}|^2 = 5\times10^{-6}$, which are not excluded for current limits [51,52]. Therefore, the effective (real) branching ratio can be written as follow

$$\begin{aligned}\mathrm{Br}_{\mathrm{eff}}^{\mathrm{Maj}} &= \epsilon\times\left(1-e^{\frac{L_D\Gamma_N^{\mathrm{Maj}}}{\gamma_N\beta_N}}\right)\times\frac{\mathrm{Br}_{\mathrm{eff}}^{\mathrm{LNC}}+\mathrm{Br}_{\mathrm{eff}}^{\mathrm{LNV}}}{\Gamma_N^{\mathrm{Maj}}} \\ &\equiv \epsilon\times\mathrm{AF}^{\mathrm{Maj}}\times\left(\frac{\mathrm{Br}_{\mathrm{eff}}^{\mathrm{LNC}}+\mathrm{Br}_{\mathrm{eff}}^{\mathrm{LNV}}}{\Gamma_N^{\mathrm{Maj}}}\right),\end{aligned} \tag{15a}$$

$$\mathrm{Br}_{\mathrm{eff}}^{\mathrm{Dir}} = \epsilon\times\left(1-e^{\frac{L_D\Gamma_N^{\mathrm{Dir}}}{\gamma_N\beta_N}}\right)\times\frac{\mathrm{Br}_{\mathrm{eff}}^{\mathrm{LNC}}}{\Gamma_N^{\mathrm{Dir}}} \equiv \epsilon\times\mathrm{AF}^{\mathrm{Dir}}\times\frac{\mathrm{Br}_{\mathrm{eff}}^{\mathrm{LNC}}}{\Gamma_N^{\mathrm{Dir}}}. \tag{15b}$$

Another important factor to take into account total detection efficiency factor ϵ which includes the estimation for tau detection. For simplicity of the detection signature, one could take only the hadronic decay channel

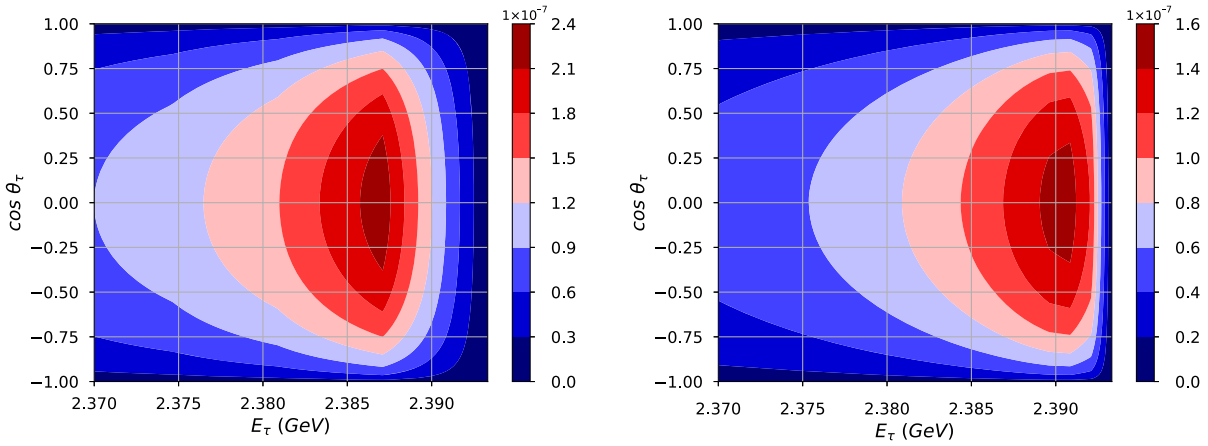

FIG. 4. Branching ratio distribution $dBr^{(X)}/dE_\tau d\cos\theta_\tau$. Left: $X =$ Dirac and Right: $X =$ Majorana. Here $m_N = 4.0$ GeV, $\epsilon = 1.0$, $|B_{\mu N}|^2 = 5 \times 10^{-7}$, and $|B_{\tau N}|^2 = 5 \times 10^{-6}$.

$\tau \to 3\pi\nu$ with a BR $\sim 9\%$ [1] and leave the other leptons to be reconstructed in the muon system, however, other hadronic decay channels must be included in order to improve the efficiency, see Refs. [53,54] for more details. We remark while for Majorana HN both channels (LNC and LNV) contribute, for Dirac ones only the LNC channel does.

III. RESULTS

In this section, we will present the results obtained through numerical solution of Eq. (15) and simulations to obtain the factor $\gamma_N\beta_N$ which are explained in detail in the Appendix. We emphasize that $\gamma_N\beta_N = 2$ has been used in all the results. Furthermore, we will focus on masses

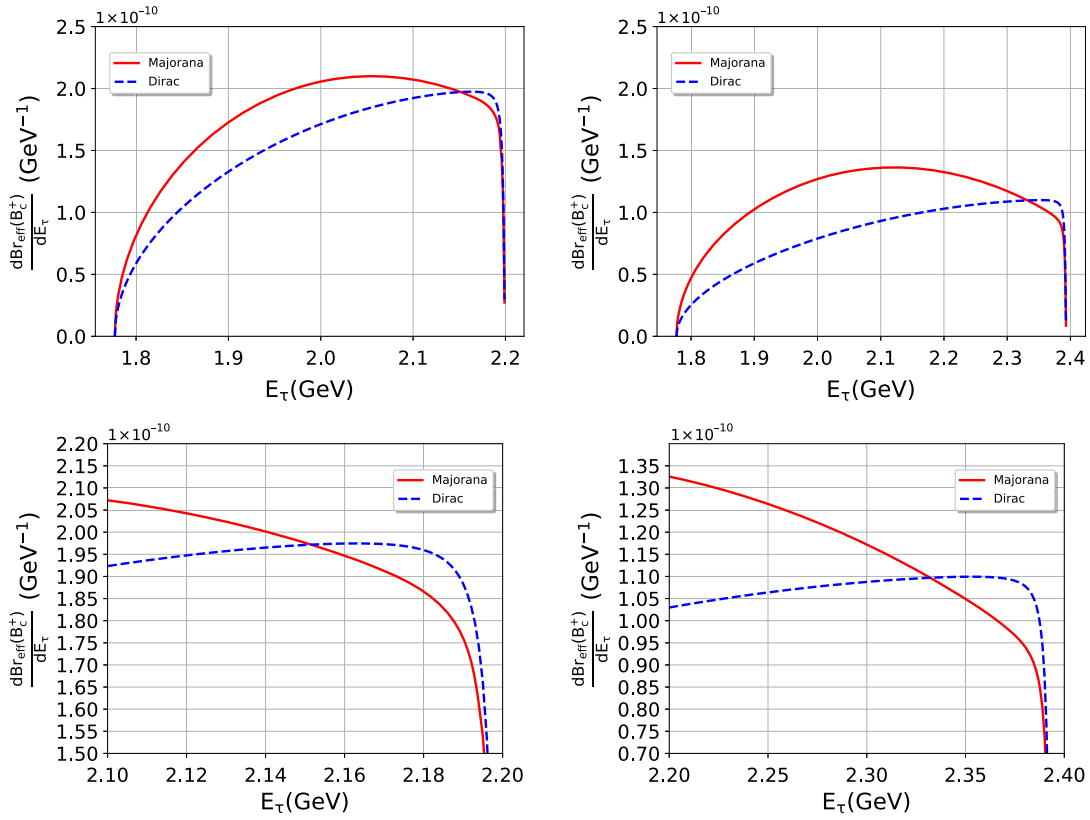

FIG. 5. Branching ratio distribution dBr/dE_τ. Top left: $m_N = 3.5$ GeV and Top right: $m_N = 4.0$ GeV. The left and right bottom panels show a zoom of pictures left and right in the top panels, respectively. Here $\epsilon = 1.0$, $|B_{\mu N}|^2 = 5 \times 10^{-7}$, and $|B_{\tau N}|^2 = 5 \times 10^{-6}$.

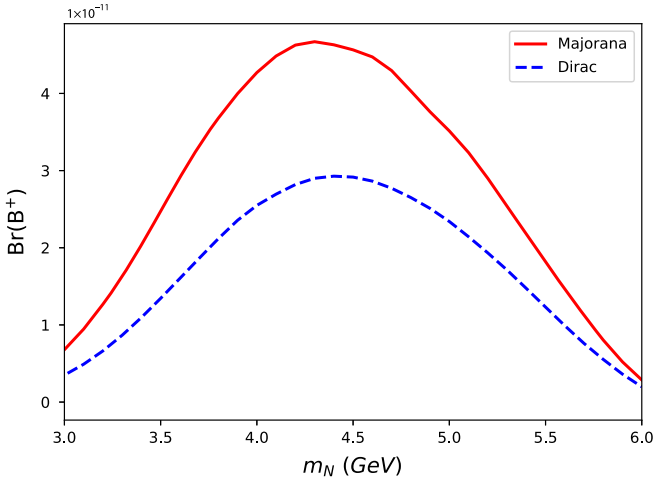

FIG. 6. Heavy neutrino effective branching ratios. The red solid line stands for the Majorana case, and the dashed blue line for the Dirac case. Here we have used $\epsilon = 0.8$, $|B_{eN}|^2 = 5 \times 10^{-7}$ and $|B_{\tau N}|^2 = 5 \times 10^{-6}$.

$m_N = 3.5$, 4.0 GeV due to these values the HN mixings $|B_{\mu N}|^2$ are less constrained from the experimental results [4,51,52].

The Fig. 4 left panel (Dirac HN) shows that the branching ratio distribution is maximum $2.1 \times 10^{-7} \leq \frac{dBr^{(\mathrm{Dir})}}{dE_\tau d\cos\theta_\tau} \leq 2.4 \times 10^{-7}$ GeV^{-1} for $2.386 \leq E_\tau \leq 2.388$ GeV and $-0.38 \leq \cos(\theta_\tau) \leq 0.38$. In the case of Fig. 4 right panel (Majorana HN) the branching ratio distribution is maximum $1.4 \times 10^{-7} \leq \frac{dBr^{(\mathrm{Dir})}}{dE_\tau d\cos\theta_\tau} \leq 1.6 \times 10^{-7}$ GeV^{-1} for $2.389 \leq E_\tau \leq 2.391$ GeV and $-0.33 \leq \cos(\theta_\tau) \leq 0.33$.

In Fig. 5 two mass cases are presented to illustrate the behavior of the branching ratio distribution $\mathrm{d}Br_{\mathrm{eff}}/dE_\tau$. In the left panel ($m_N = 3.5$ GeV) is possible to observe that in the range $1.77 \leq E_\tau \leq 2.15$ GeV of the energy the Majorana case dominates over Dirac. On the contrary in the $2.15 \leq E_\tau \leq 2.19$ GeV range the Dirac dominates over Majorana. Similarly, for Neutrino masses of 4.0 GeV (right panel), the Majarona dominates in the $1.77 \leq E_\tau \leq 2.33$ GeV HN mass range and Dirac on the $2.33 \leq E_\tau \leq 2.39$ GeV range, however, the difference in the slope between Majorana and Dirac is more evident.

In order to estimate a realistic number of HN that can be produced at the HL-LHCb, we will consider the detector efficiency $\epsilon = 0.8$, which is under a conservative approach [55]. Therefore, in Fig. 6 we present the values of effective branching ratios [Eq. (15)] over our range of interest for heavy neutrino masses ($3 \lesssim m_N \lesssim 6$ GeV) for the above mentioned efficiency. On the other hand, considering a luminosity of about $\mathcal{L} = 10^{34}$ cm^{-2} sec^{-1}, one could expect the total amount of B_c mesons produced of the order of $N_{B_c} \sim 5 \times 10^{10}$ per year [56]. In Table I we show the expected number of HN N_N^X ($X = \mathrm{Dir/Maj}$) for the two HN studied masses ($m_N = 3.5$, 4.0), and for the two HN nature (Dirac and Majorana).

TABLE I. Expected number of HN at HL-LHCb with an overall detector efficiency of 0.8. Here we have used $|B_{\mu N}|^2 = 5 \times 10^{-7}$ and $|B_{\tau N}|^2 = 5 \times 10^{-6}$.

m_N (GeV)	Operation time (years)	Br^{Dir}	N_N^{Dir}	Br^{Maj}	N_N^{Maj}
3.5	5	1.34×10^{-11}	≈3	2.47×10^{-11}	≈6
3.5	10	1.34×10^{-11}	≈7	2.47×10^{-11}	≈12
3.5	15	1.34×10^{-11}	≈11	2.47×10^{-11}	≈19
4.0	5	2.55×10^{-11}	≈6	4.27×10^{-11}	≈11
4.0	10	2.55×10^{-11}	≈13	4.27×10^{-11}	≈21
4.0	15	2.55×10^{-11}	≈19	4.27×10^{-11}	≈32

IV. SUMMARY AND CONCLUSIONS

In this work, we have studied the production of HN's via the rare B_c meson decay $B_c^+ \to \mu^+ N \to \mu^+\mu^+\tau^-\nu$ in the HL-LHCb experiment. We have shown that for mixings elements $|B_{\mu N}|^2 = 5 \times 10^{-7}$ and $|B_{\tau N}|^2 = 5 \times 10^{-6}$ and for HN masses $m_N = 3.5$ and $m_N = 4.0$ GeV would be possible to probe the existence of HN during the LHC-LHCb lifetime. It is worth mentioning, that we focus on a scenario with conservative values for HN mixing elements $|B_{\ell N}|$, however, there are scenarios where the HN mixings elements are less tighten $|B_{\mu N}|^2 \sim 10^{-6}$ and $|B_{\tau N}|^2 \sim 10^{-5}$ which allows producing up to 3000 HN events for Majorana case [45]. Furthermore, we emphasize that due to the different energy distributions of the final tau lepton (Fig. 5), it could be possible to reveal the HN's nature. In addition, the angular distribution (Fig. 4) between final leptons might be the key to improving the signature of the events and unveiling the Dirac and Majorana cases.

ACKNOWLEDGMENTS

The work of J. Z.-S. was funded by ANID-Millennium Science Initiative Program—ICN2019_044. The work of G. V. is supported by the Natural Science and Engineering Research Council, Canada.

APPENDIX

An appropriate evaluation of Eq. (15) requires a realistic value of $\gamma_N\beta_N$, which can be obtained from the $\gamma_{B_c^+}$ distribution by means of Lorentz transformation. The $\gamma_{B_c^+}$ distribution is presented in Fig. 7 and was obtained carrying out simulations of B_c^+ mesons production via charged current Drell-Yan process, using MadGraph5_aMC@NLO [57], PYTHIA8 [58], and DELPHES [59], for the LHCb conditions at $\sqrt{s} = 13$ TeV. The B_c^+ meson velocity ($\equiv\beta_{B_c^+}$) can be obtained from $\gamma_{B_c^+}$ using $\beta_{B_c^+} = \sqrt{1 - 1/\gamma_{B_c^+}^2}$. The Fig. 7 show the $\gamma_{B_c^+}$ distribution.

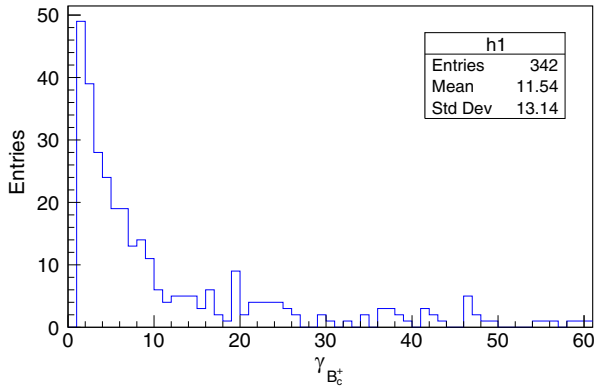

FIG. 7. The $\gamma_{B_c^+}$ distribution. We notice that the most representative value is $\gamma_{B_c^+} = 2.0$.

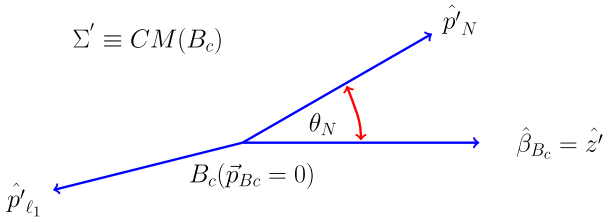

FIG. 8. Schematics representation of the directions of 3-momentum in the B_c^+-rest frame (Σ'). Here θ_N is the angle which define the angle between $\hat{\beta}_{B_c^+}$ and $\hat{p}'_N$, where $\hat{\beta}_{B_c^+} = \frac{\vec{\beta}_{B_c^+}}{|\vec{\beta}_{B_c^+}|}$ is the direction of the velocity of B_c^+ in the lab frame. For simplicity we will consider that $\hat{\beta}_{B_c^+}$ also defines the $\hat{z}'$-axis.

It is worth mentioning, that, in general, B_c^+ is moving when it decays into N and ℓ_1, therefore, the product $\gamma_N\beta_N$ is not always fixed and can be written in the CM(N) frame as

$$\beta_N\gamma_N = \sqrt{(E_N(\hat{p}'_N)/m_N)^2 - 1}, \tag{A1}$$

where E_N is the heavy neutrino energy in the CM(N) frame, and $\hat{p}'_N$ is the direction of the heavy neutrino in the B_c^+-rest frame (Σ').

TABLE II. The values of $\gamma_N\beta_N$ for $\gamma_{B_c^+} = 2.0$, $\beta_{B_c^+} = 0.75$ and different angles θ_N. The average value for $m_N = 3.5$ GeV is $\gamma_N\beta_N = 2.01$, while for $m_N = 4.0$ GeV is $\gamma_N\beta_N = 1.94$.

m_N (GeV)	θ_N (rad)	$\gamma_N\beta_N$
3.5	0	3.12
3.5	$\pi/2$	2.13
3.5	π	1.01
4.0	0	2.73
4.0	$\pi/2$	1.97
4.0	π	1.13

The relation among E_N, $\overrightarrow{p'}_N$ and the angle θ_N is given by the Lorentz energy transformation (see Fig. 8)

$$E_N = \gamma_{B_c^+}(E'_N + \cos\theta_N\beta_{B_c^+}|\vec{p}'_N|), \tag{A2}$$

where the corresponding factors in the B_c^+-rest frame (Σ') are given by

$$E'_N = \frac{m_{Bc}^2 + m_N^2 - m_{\ell_1}^2}{2m_{Bc}}, |\overrightarrow{p'}_N| = \frac{1}{2}m_{Bc}\lambda^{1/2}\left(1, \frac{m_{\ell_1}^2}{m_{Bc}^2}, \frac{m_N^2}{m_{Bc}^2}\right), \tag{A3}$$

we remarks that β_{Bc} is the velocity of B_c^+ in the lab frame, and $\lambda(x, y, z)$ is

$$\lambda(x, y, z) = x^2 + y^2 + z^2 - 2xy - 2xz - 2yz. \tag{A4}$$

It is worthwhile to notice that the $\gamma_N\beta_N$ values can range between the values presented in Table II. Therefore, to perform the calculation in a simple way, during the development of this work we have considered $\gamma_N\beta_N = 2.0$, however, we stress that the result does not change significantly in the range $1.01 \leq \gamma_N\beta_N \leq 3.12$.

[1] R. L. Workman *et al.* (Particle Data Group), Prog. Theor. Exp. Phys. **2022**, 083C01 (2022).
[2] R. N. Mohapatra *et al.*, Rep. Prog. Phys. **70**, 1757 (2007).
[3] R. N. Mohapatra and A. Y. Smirnov, Annu. Rev. Nucl. Part. Sci. **56**, 569 (2006).
[4] A. Atre, T. Han, S. Pascoli, and B. Zhang, J. High Energy Phys. 05 (2009) 030.
[5] C. Dib, V. Gribanov, S. Kovalenko, and I. Schmidt, Phys. Lett. B **493**, 82 (2000).
[6] G. Cvetic, C. Dib, and C. S. Kim, J. High Energy Phys. 06 (2012) 149.
[7] G. Cvetic, C. Kim, and J. Zamora-Saa, J. Phys. G **41**, 075004 (2014).
[8] G. Cvetic, C. Kim, and J. Zamora-Saa, Phys. Rev. D **89**, 093012 (2014).
[9] G. Cvetic, C. Dib, C. S. Kim, and J. Zamora-Saa, Symmetry **7**, 726 (2015).
[10] G. Cvetic, C. S. Kim, R. Kogerler, and J. Zamora-Saa, Phys. Rev. D **92**, 013015 (2015).

[11] C. O. Dib, M. Campos, and C. Kim, J. High Energy Phys. 02 (2015) 108.
[12] G. Moreno and J. Zamora-Saa, Phys. Rev. D **94**, 093005 (2016).
[13] D. Milanes and N. Quintero, Phys. Rev. D **98**, 096004 (2018).
[14] J. Mejia-Guisao, D. Milanes, N. Quintero, and J. D. Ruiz-Alvarez, Phys. Rev. D **97**, 075018 (2018).
[15] G. Cvetic, C. S. Kim, S. Mendizabal, and J. Zamora-Saa, Eur. Phys. J. C **80**, 1052 (2020).
[16] A. Abada, C. Hati, X. Marcano, and A. M. Teixeira, J. High Energy Phys. 09 (2019) 017.
[17] T. Asaka and H. Ishida, Phys. Lett. B **763**, 393 (2016).
[18] A. Das, S. Jana, S. Mandal, and S. Nandi, Phys. Rev. D **99**, 055030 (2019).
[19] A. Das and N. Okada, Phys. Lett. B **774**, 32 (2017).
[20] A. Das and N. Okada, Phys. Rev. D **88**, 113001 (2013).
[21] S. Antusch, E. Cazzato, and O. Fischer, Mod. Phys. Lett. A **34**, 1950061 (2019).
[22] A. Das, Y. Gao, and T. Kamon, Eur. Phys. J. C **79**, 424 (2019).
[23] A. Das, P. S. B. Dev, and C. S. Kim, Phys. Rev. D **95**, 115013 (2017).
[24] S. Chakraborty, M. Mitra, and S. Shil, Phys. Rev. D **100**, 015012 (2019).
[25] G. Cvetic and C. S. Kim, Phys. Rev. D **100**, 015014 (2019).
[26] S. Antusch, E. Cazzato, and O. Fischer, Int. J. Mod. Phys. A **32**, 1750078 (2017).
[27] G. Cottin, J. C. Helo, and M. Hirsch, Phys. Rev. D **98**, 035012 (2018).
[28] L. Duarte, G. Zapata, and O. A. Sampayo, Eur. Phys. J. C **79**, 240 (2019).
[29] M. Drewes and J. Hajer, J. High Energy Phys. 02 (2020) 070.
[30] P. S. Bhupal Dev, R. N. Mohapatra, and Y. Zhang, J. High Energy Phys. 11 (2019) 137.
[31] G. Cvetič, A. Das, and J. Zamora-Saá, J. Phys. G **46**, 075002 (2019).
[32] G. Cvetič, A. Das, S. Tapia, and J. Zamora-Saá, J. Phys. G **47**, 015001 (2020).
[33] A. Das, Adv. High Energy Phys. **2018**, 9785318 (2018).
[34] A. Das, P. Konar, and S. Majhi, J. High Energy Phys. 06 (2016) 019.
[35] A. Das, P. S. B. Dev, and R. N. Mohapatra, Phys. Rev. D **97**, 015018 (2018).
[36] A. Abada, P. Escribano, X. Marcano, and G. Piazza, Eur. Phys. J. C **82**, 1030 (2022).
[37] A. Abada, N. Bernal, M. Losada, and X. Marcano, J. High Energy Phys. 01 (2019) 093.
[38] E. Arganda, M. J. Herrero, X. Marcano, and C. Weiland, Phys. Lett. B **752**, 46 (2016).
[39] J. Zamora-Saa, J. High Energy Phys. 05 (2017) 110.
[40] C. S. Kim, G. López Castro, and D. Sahoo, Phys. Rev. D **96**, 075016 (2017).
[41] C. O. Dib, J. C. Helo, M. Nayak, N. A. Neill, A. Soffer, and J. Zamora-Saa, Phys. Rev. D **101**, 093003 (2020).
[42] T. Asaka, S. Blanchet, and M. Shaposhnikov, Phys. Lett. B **631**, 151 (2005).
[43] T. Asaka and M. Shaposhnikov, Phys. Lett. B **620**, 17 (2005).
[44] E. K. Akhmedov, V. A. Rubakov, and A. Y. Smirnov, Phys. Rev. Lett. **81**, 1359 (1998).
[45] S. Tapia, M. Vidal-Bravo, and J. Zamora-Saa, Phys. Rev. D **105**, 035003 (2022).
[46] R. Aaij *et al.* (LHCb Collaboration), Nat. Phys. **18**, 1 (2022).
[47] R. Aaij *et al.* (LHCb Collaboration), J. High Energy Phys. 03 (2021) 075.
[48] G. Cvetic, C. S. Kim, G.-L. Wang, and W. Namgung, Phys. Lett. B **596**, 84 (2004).
[49] J. Beringer *et al.* (Particle Data Group), Phys. Rev. D **86**, 010001 (2012).
[50] P. J. Mohr, B. N. Taylor, and D. B. Newell, Rev. Mod. Phys. **84**, 1527 (2012).
[51] I. Boiarska, A. Boyarsky, O. Mikulenko, and M. Ovchynnikov, Phys. Rev. D **104**, 095019 (2021).
[52] A. M. Abdullahi *et al.*, J. Phys. G **50**, 020501 (2023).
[53] D. Acosta *et al.*, arXiv:2110.14675.
[54] R. Aaij *et al.* (LHCb Collaboration), LHCb trigger and online upgrade technical design report, Technical Reports No. CERN-LHCC-2014-016, No. LHCB-TDR-016, 2014, https://cds.cern.ch/record/1701361.
[55] LHCb Collaboration, J. Instrum. **10**, P02007 (2015).
[56] I. P. Gouz, V. V. Kiselev, A. K. Likhoded, V. I. Romanovsky, and O. P. Yushchenko, Phys. At. Nucl. **67**, 1559 (2004).
[57] J. Alwall, R. Frederix, S. Frixione, V. Hirschi, F. Maltoni, O. Mattelaer, H. S. Shao, T. Stelzer, P. Torrielli, and M. Zaro, J. High Energy Phys. 07 (2014) 079.
[58] T. Sjostrand, S. Mrenna, and P. Z. Skands, Comput. Phys. Commun. **178**, 852 (2008).
[59] J. de Favereau, C. Delaere, P. Demin, A. Giammanco, V. Lemaître, A. Mertens, and M. Selvaggi (DELPHES 3 Collaboration), J. High Energy Phys. 02 (2014) 057.